Omics Insights into Metabolic Stress and Resilience of Rats in Response to Short-term Fructose Overfeeding

Kun-Ping Li[a,b], Min Yuan[a,b], Zhuo-Ru He[a,b], Qi Wu[a,e], Chu-mei Zhang[a,b], Zhi-Li Lei[a,e], Xiang-Lu Rong[a,e], Zebo Huang [c], Jeremy E. Turnbull[d*], Jiao Guo[a,e*]

a.Institute of Chinese Medicinal Sciences, Guangdong Pharmaceutical University, Guangzhou 510006, China

b.School of Pharmacy, Guangdong Pharmaceutical University, Guangzhou 510006, China.

c.School of Food Science and Engineering, South China University of Technology, Guangzhou 510006, China.

d.Centre for Glycobiology, Department of Biochemistry, Institute of Integrative Biology, University of Liverpool, Liverpool L69 7ZB, England, UK.

e.Guangdong Metabolic Disease Research Center of Integrated Medicine, Guangzhou, 510006, China.

*Corresponding Authors:

Prof. Jiao Guo

Institute of Chinese Medicinal Sciences,

Guangdong Pharmaceutical University

280 East Road, Outer Ring, Guangzhou Higher Education Mega Center, Guangzhou, China (510006)

Tel: + 86-20-39352818; Fax: +86-20-39352818; E-mail: gyguoyz@163.com

Prof. Jeremy Turnbull

Centre for Glycobiology, Department of Biochemistry

University of Liverpool, Liverpool L69 7ZB, UK

Tel: +44 151 795 4427; E-mail: j.turnbull@liverpool.ac.uk

Abstract

Scope Considerable evidence supports the view that high-fructose intake is associated with increased and early incidence of obesity and dyslipidemia. However, knowledge on physiopathological alterations introduced by fructose overconsumption is lacking. We have therefore carried out an integrated omics analysis to investigate the consequences of short-term fructose overfeeding(SFO) and identify the underlying molecular mechanisms.

Methods and results SFO of rats demonstrated obvious histopathological hepatic lipid accumulation and significant elevation in adiposity, total cholesterol and fasting plasma glucose levels. Integrated omics analysis demonstrated that SFO disturbed metabolic homeostasis and initiated metabolic stress. Hepatic lipogenesis pathways were also negatively impacted by SFO. Analysis of molecular networks generated by IPA implicated involvement of the ERK signaling pathway in SFO and its consequences. Moreover, we identified that an inherent negative feedback regulation of hepatic SREBP1 plays an active role in regulating hepatic *de novo* lipogenesis.

Conclusion Our findings indicate that SFO disturbs metabolic homeostasis and that endogenous small molecules positively mediate SFO induced metabolic adaption. Our results also underline that an inherent regulatory mechanism of resilience occurs in response to fructose overconsumption, suggesting that efforts to maintain resilience could be a promising target to prevent and treat metabolic disorder-like conditions.

Key words: short-term fructose overfeeding, metabolomics, RNA-Seq, SREBP-1, resilient regulation

Highlight:

1. Short-term fructose overfeeding (SFO) has noteworthy impacts on rats' hepatic gene expression.
2. Dyslipidemia, obesity and diabetes are likely consequential conditions of SFO.
3. A self-adaptive metabolic regulation is an inherent resilience response to SFO.
4. Negative feedback regulation of SREBP-1 partly mediates the SFO metabolic adaptation.

Abbreviations:

SFO	short-term fructose overfeeding
IPA	Ingenuity Pathways Analysis
DEGs	differentially expressed genes
DMs	different metabolites
NTMA	non-targeted metabolomics analysis
QTLA	quantitative targeted lipidomics analysis
PCA	principle component analysis
OPLS-DA	orthogonal partial least squares- discriminant analysis
ERK	extracellular signal regulated kinase
SREBP-1	sterol regulatory element binding protein-1
CHREBP	carbohydrate responsive-element binding protein
FFAs	free fatty acids
MUFA	monounsaturated fatty acids
PUFA	polyunsaturated fatty acids

1 Introduction

Nowadays, obesity and dyslipidemia are more popular than ever in human history. One of the accepted explanations to its increase and early incidence is over nutrition and lack of physical activity which are key elements of overweight and obesity, and the dietary pattern including a fat and fructose rich diet are thought to be critical, too [1, 2]. High fructose corn syrup (HFCS), a sweetener made from corn starch, is widely used in food products and beverages. Although a gradual decrease in the consumption rate has been apparent in the past few years, fructose consumption has gradually increased in Western countries [3]. This increasing rate of caloric intake from high-fructose containing food and beverages is considered to be a contributory factor to increased dyslipidemia and obesity in developed countries [1, 4, 5].

In fact, ample epidemiological and experimental evidence supports that high-fructose intake could be a risk factor for dyslipidemia, insulin resistance, obesity, and type 2 diabetes [6, 7]. Therefore, social concern regarding disorders of fructose metabolism has been growing for the last decade in developing countries. However, the consequences of short-term fructose overfeeding (SFO) on body metabolism has not yet been fully investigated from an omics viewpoint, including its related phenotypes and underlying pathogenic mechanisms. Although the fructose overfeeding animal model is often used for related physiopathological and pharmacological research, omics knowledge on fructose overconsumption is lacking.

Omics analysis, especially integrated transcriptomics and metabolomics analysis, are emerging as robust tools for studies on diagnostic biomarkers, fundamental pathogenic mechanisms and therapeutic targets [8-12]. According to the biochemical understanding, transcripts and metabolites are intermediates and end products respectively, which can reflect alterations of the bodies homeostasis at

two distinctive levels. Moreover, combined with IPA(Ingenuity Pathways Analysis), MetaCore(GeneGo) , Reactome (https://reactome.org/) or some other pathway analysis programs , the algorithmically constructed metabolic networks and gene expression networks can generate much more insight than phenotypes and results analyzed individually [13-15].

In the present study, we firstly performed RNA-Seq based hepatic transcriptome analysis to investigate the alteration of hepatic gene expression patterns resulting from SFO. Following the transcriptomics sequential hits, we then carried out both non-targeted metabolomics and quantitative targeted lipidomic analysis of rat plasma. Finally, using molecular networks generated from the omics discoveries and Ingenuity Pathway Analysis, we evaluated the impacts of SFO on rat metabolic homeostasis. The results revealed that hepatic gene expression networks were significantly impacted, inducing responses resulting in dyslipidemia, with predicted downstream consequences of obesity and diabetes. However, a resilient self-adaptive metabolic regulation mechanism was also noted. Our results also provide abundant omics information for SFO rats that will be very useful for understanding resulting pathogenic mechanisms and research on therapeutic strategies for early-onset dyslipidemia and obesity.

2 Materials and Methods

2.1 Reagents

D-Fructose was from Amresco (Solon, Ohio, USA). Nonadecanoic acid and F.A.M.E. Mix (C4-C24) were from Sigma-Aldrich (San Diego, CA, USA). Meth-Prep II was from Grace (Grace Discovery Sciences, MD, USA). Methanol, hexane and chloroform were of HPLC grade and were from Merck (Darmstadt, German). All the derivatization agents for GC-MS based metabolomics

analysis were supplied by J&K scientific Co. Ltd (Tianjing, China).

2.2 Animals

The experimental protocols and procedures for animal care were approved by the Institutional Animal Care and Use Committee of the Guangdong Pharmaceutical University. 5-week-old male Sprague-Dawley rats (171±7.7 g) were supplied by Guangdong Medical Laboratory Animal Center and housed in environmentally controlled conditions at room temperature (24℃± 3 ℃) under a 12:12 h light-dark cycle. After acclimatization for 5 days, the animals were divided into two groups: the control group (con, n=6) and the short-term fructose overfeeding group (SFO, n=6). The former received standard rodent chow and drinking water while the latter received standard rodent chow and a 20% fructose aqueous solution. The fructose overfeeding experiment lasted for 16 days. All the animals received their respective food and drinks *ad libitum*. The amount of consumed chow, the volume of consumed water and 20% fructose solution of each group were recorded every day for calculating the energy intake.

2.3 Sample collection

At the end of the experiment, the rats were fasted overnight (16 h), and then all the rats were anaesthetized with pentobarbital sodium to collect the blood and liver samples. The blood was centrifuged at 3000 rpm for 10 min to obtain the plasma which was then aliquoted into 1.5 mL Eppendorf tubes and flash frozen for later biochemical analysis and metabolomics analysis. The livers were washed by saline, and parts of them were fixed with 4% PFA(Paraformaldehyde) for histological examination. All the other liver tissues were flash frozen in liquid nitrogen for RNA-Seq.

2.4 Rats' body and adiposity

Body weight of rats were collected every two days. Fat weight of rats were measured by using the Minispec LF90II body composition analyzer (Bruker Optics, Billerica, MA, USA) on day 0, 8 and 16[16]. The adiposity was calculated as adiposity = Fat weight / Body weight.

2.5 Plasma biochemical analysis

Triglyceride, total cholesterol (TC), low-density lipoprotein cholesterol (LDL-C) and high-density lipoprotein cholesterol (HDL-C) of the rats' plasma were measured using corresponding commercial assay kits (Nanjing Jiancheng Bioengineering Institute, China). Plasma non-fasting glucose (NFG) collected on day 14 by periorbital puncture and fasting glucose (FG) collected from the abdominal aorta on the last day were determined using an ELISA kit (CUSABIO, Wuhan, China).

2.6 Histological examinations of hepatic tissues

Routine hematoxylin and eosin (H&E) staining of liver tissues were carried out using 4% PFA fixing, paraffin embedding and sectioning (5 μm) as described previously [17]. Three or four sections from every tissue sample were chosen for staining. An Olympus BX53 microscope and imaging system was used. Oil red O staining was performed to analyze fat accumulation in the rat liver and the liver infarcted areas were analyzed using image J software(NIH, Maryland, USA) [13].

2.7 Transcriptome analysis

Total RNA was extracted from liver with the Trizol Kit (Promega, USA) following by the manufacturer's instructions. cDNA library was constructed and then sequenced on the Illumina sequencing platform (Illumina HiSeq™ 4000) using the paired-end technology by Gene Denovo Co. (Guangzhou, China). All the transcriptome reads were submitted to GenBank's Sequence Read Archive (access numbers SRR6656395, SRR6656396, SRR6656397, SRR6656398, SRR6656393 and

SRR6656394). Differential gene expression patterns were analyzed for annotated genes between the two groups using fragments per kilobase of transcript per Million mapped reads (FPKM) values. Differentially expressed genes (DEGs) were screened out by using the false discovery rate (FDR) *p*-values < 0.05 and $|\log_2 FC|>1$ as the threshold; which were then subjected to pathway enrichment analysis.

2.8 Metabolomics analysis

Non-targeted metabolomics analysis (NTMA) and quantitative targeted lipidomics analysis (QTLA) of plasma were performed as described previously [17]. In brief, all the GC-MS raw data were executed batch molecular feature extraction by using MassHunter Profinder_B.08(Agilent Co., Ltd, CA, USA). Then, the generated data were exported to Excel (Microsoft, Redmond, WA, USA) which were used in the subsequent multivariate analysis. All the raw data were stored at Guangdong Metabolic Disease Research Centre of Integrated Medicine, which will be available upon requested. Unsupervised PCA and supervised OPLS-DA analysis were performed on SIMCA-P 13.0 software (Umetrics, Umeå, Sweden) to identify plasma metabolites contributing to the differences between the two groups. All variables were Pareto-scaled prior to analyses. Here, VIP (Variable Importance in Projection) >1.0 and $p < 0.05$ were set as a statistical threshold for discriminating significantly different metabolites (DMs).

2.9 Systematic molecular network analysis

Systematic molecular network analysis was carried out with Ingenuity Pathway Analysis (IPA, http://www.ingenuity.com) and MetaboAnalyst 3.0 (http://www.metaboanalyst.ca/) [17, 18]. Identified DEGs and DMs were submitted to elucidate gene networks and/or possible biological functions.

Systematic molecular networks were generated based on the knowledge sorted in the Ingenuity Pathway Knowledge Base and Kyoto Encyclopedia of Genes and Genomes (KEGG; http://www.genome.jp/kegg/) and the Human Metabolome Database (HMDB; http://www.hmdb.ca/). The network score was based on the hypergeiometric distribution and was calculated with the right-tailed Fisher's Exact Test. The higher the score, the more relevant the molecules and genes were to the network.

2.10 Quantitative real-time PCR

qRT-PCR was performed on PikoReal^{TM} Real-Time PCR System (Thermo Scientific, USA). The liver tissue total RNA was extracted with Trizol RNA Kit (TaKaRa, Japan). cDNA was synthesized using the PrimeScript RT reagent kit with gDNA Eraser (TaKaRa, Japan). STBR® Premix Ex Taq^{TM} II (TaKaRa, Japan) was used for qPCR with specific primers suitable for different genes, following the manufacturer's protocol. Several key genes involved in hepatic lipogenesis were selected to validate the expression patterns while β-actin gene was used as an internal control. The relative expression fold change was calculated by the $2^{-\Delta\Delta Ct}$ comparative threshold cycle method.

2.11 Western blotting

Western blotting was conducted as previous described, protein concentration was determined by BCA method[16]. Briefly, protein content was separated on SDS-PAGE and transferred to PVDF membrane. The membrane was then blocked with 5% non-fat milk at room temperature for 2 h, following incubation with the primary antibodies against SREBP1(Rabbit polyclonal ab28481, Abcam, Cambridge,UK), SREBP2(Rabbit polyclonal ab28481, Abcam, Cambridge,UK) and ChREBP(Rabbit polyclonal ab92809, Abcam, Cambridge, UK) at 4 ℃ overnight. Subsequently, the membrane was incubated with appropriated HRP-conjugated secondary antibody (Cell Signaling Technology, Boston, MA) for 1 hour. β-actin (Invitrogen™, Carlsbad, CA) was used as loading control. Target bands were

developed using a chemiluminescence system and the intensity of the immunoblot signal was detected using Western Bright™ ECL spray and quantitatively evaluated using GeneTools software from Syngene (Cambridge, UK).

2.12 Statistical analysis

All data are expressed as means ± standard deviation (SD). R (https://www.r-project.org) and Graphpad Prism 6.0 software (GraphPad, CA, USA) were used for statistical analysis and graphics. For metabolomics analysis, data were normalized to the internal standard and all variables were Pareto-scaled prior to analyses. A two-tailed Student's t-test was performed except for adiposity analysis (2-way ANOVA test). $p < 0.05$ was considered statistically significant.

3 Results

3.1 Short-term fructose overfeeding accelerated dyslipidemia and hepatic lipid accumulation

We first evaluated physiological responses to short-term fructose overfeeding (SFO) for 16 days. As shown in Figure 1 A&B, compared to the control group, the body weight of SFO rats increased steadily at a higher rate (Fig. 1A), and body fat rates in SFO rats were also elevated significantly by day 8, and maintained at this higher level at day 16 ($p<0.05$) (Fig. 1 B). The levels of total cholesterol (TC) and fasting glucose in rats' plasma showed an obvious rise in the SFO group ($p<0.05$; Figure 1C, D). The levels of plasma triglyceride, and low-density lipoprotein cholesterol (LDL-C) as well as high-density lipoprotein cholesterol (HDL-C) in SFO rats showed a trend towards increased levels but this was not statistically significant (Figure 1C). Thus the effects of fructose overfeeding for 16 days was predominantly noted on cholesterol and glucose metabolism. Furthermore, histological analyses of stained liver tissues by Oil Red O (O.R.O.) staining demonstrated clear evidence of fat infiltration in SFO rats (Figure 1E); this was confirmed by quantitation of the results, where a statistically significant

change in O.R.O. stained plaque area between the two groups (p<0.01; Figure 1F). Moreover, hepatic triglyceride in SFO rats showed a significant increase (Figure 1G). Collectively these data demonstrate that SFO results in rapid onset of dyslipidemia and hepatic lipid accumulation in rats.

3.2 Transcriptomics analysis revealed that disturbed hepatic gene expression patterns result from short-term fructose overfeeding

Fructose has been reported to be a lipogenic substance and potent inducer of lipogenic enzyme expression [19]. We undertook a transcriptomic analysis of gene expression in liver tissue from control and SFO rats. A total of 20.6 Gb high quality clean reads were generated and 16087 and 16283 transcripts were aligned to the reference genome (*Rattus norvegicus* Rnor_6.0) in control and SFO groups, respectively. As a result, 64 up-regulated and 41 down-regulated differentially expressed genes (DEGs) were uncovered; among these, the metabolism related DEGs are listed in Table S1 (in Supplementary Information). In the GO classification (Figure 2), the top three enriched up-regulated biological processes were metabolic, cellular and single-organism processes, while biological regulation, cellular processes and single-organism processes were the top three enriched down-regulated processes. Meanwhile, pancreatic secretion, protein digestion and absorption, and fat digestion and absorption were the top three KEGG enrichment pathways for differentially expressed genes (Figure 3). Referring to the known pathways in the KEGG database, the schematic downstream *de novo* lipogenesis pathway and acyl-generating pathway in liver cell are illustrated in Figure 4A and C, respectively, with corresponding heatmaps of gene expression data shown in Figure 4B and D. These expression data were generated based on the RNA-Seq presented FPKM value of each gene. In both Figure 4B and D, the control and SFO groups display distinct expression patterns, while there existed a consistently high level of gene expression in the SFO group for a number of key enzymes.

Validation of the RNA-Seq data was undertaken by qRT-PCR of several genes involved in hepatic lipogenesis (Figure 4E). These results are consistent with the conclusion that SFO results in robust stimulation of hepatic *de novo* lipogenesis and acyl-generating pathways, resulting in elevated hallmarks of dyslipidemia (Fig. 1).

3.3 Metabolomics analysis revealed significant alterations in lipid and energy metabolism after short-term fructose overfeeding

To investigate further potential changes in metabolites which might underly the effects of SFO, we performed metabolomics analysis on plasma samples, hypothesizing that transcriptome and plasma metabolome may demonstrate related alterations. Based on the acquired non-targeted metabolomics analysis (NTMA) and quantitative targeted lipidomics analysis (QTLA), the data provided abundant qualitative and quantitative information demonstrating altered endogenous metabolites. For the NTMA (Figure 5A&B), 198 molecules were unequivocally identified and 30 of them were regarded as significantly different metabolites (DMs; see Table S2 in Supplementary Information). The pathway analysis of these DMs with MetaboAnalyst 3.0 showed that aminoacyl-tRNA biosynthesis, primary bile acid biosynthesis, galactose metabolism are the top three enriched pathways based on the hit molecules (Figure 5C; a,b and c). In addition, results from enrichment analysis of the disease-associated metabolites set (30 metabolites) demonstrated that diabetes mellitus was the top likely resulting disease (Figure 5D). In more detail, there were seven metabolites enriched as linked to the likely disease of diabetes mellitus, including 3-hydroxybutyric acid, creatinine, taurine, L-glutamine, citric acid, D-glucose and L-tryptophan. Regarding the QTLA, 36 fatty acids in plasma were quantitatively profiled and the resulting heatmap is shown in Figure 5E. Compared with the control group, the content of most fatty acids are elevated in SFO rats, especially the unsaturated fatty acids,

including C16:1, C18:1n9c, C18:2n6c, C22:6n3, C20:3n3 and C20:4n6 (Figure 5F). The relative levels of polyunsaturated fatty acids (PUFA) and monounsaturated fatty acids (MUFA) in SFO rats were much higher than that in the control group; for example, the relative level of C20:4n6 and C22:6n3 reached almost 120 and 80 fold, respectively. Moreover, the levels of the n3 and n6 fatty acids are also increased, but the former increases more than the latter. A similar situation occurs on the *cis*- and *trans*-fatty acids (Figure 5F). Interestingly, after normalization to the total fatty acids, the relative content of *cis*-fatty acids was higher in the SFO group, with the *trans*-fatty acids being lower than in the control group (Figure 5E).

3.4 Short-term fructose overfeeding stresses glycolipid metabolism related pathways

From the above-mentioned transcriptomics and metabolomics analyses, it was demonstrated that an obvious metabolic stress was initiated by SFO. To further illustrate and visualize the underlying metabolic stress induced by SFO, the above-mentioned DEGs and DMs were further analyzed using Ingenuity Pathways Analysis [20] software to interpret the apparently independent changes into altered canonical pathways and gene regulation networks. As a result, two molecular networks were generated for metabolites (Figure 6; IPA scores, 47) and for differential gene expression (Figure 7A; IPA scores, 40). The top metabolic network, which involved 19 molecules in our listed DMs, highlighted a marked connection with proinsulin, low-density lipoprotein (LDL), high-density lipoprotein (HDL), nitric oxide synthase, superoxide dismutase (Sod), extracellular signal regulated kinase 1 and 2 (ERK1/2), and growth hormone (Figure 6). The gene expression network, which involved 16 proteins in our listed DEGs, highlighted connections between insulin, ERK1/2, phosphatidyl inositol 3-kinase (PI3K), and protein kinase B (Akt) (Figure 7A). Both of these analyses underscored that the ERK signaling pathway, a known glycolipid metabolism related pathway, was a major nexus shouldering significant metabolic

stress associated with SFO. In addition, an intensive sub-network (Figure 7B), focused on 4 key elements related to glycolipid metabolism, namely metabolism of triacylglycerol, fatty acid metabolism, synthesis of fatty acid and synthesis of lipids, demonstrated obvious metabolic dysregulation, with a predicted increase in obesity as a likely consequence.

3.5 Resilient regulation alleviated metabolic stress induced by short-term fructose overfeeding

Accurate regulation of levels of all kinds of endogenous molecules is critical for cellular and organismal homeostasis. Self-adaptive metabolic regulation is inherent for mammals facing biotic or abiotic stress [21]. A quantitative annotated basic metabolism network (see Figure S1 in supplementary Information) after short-term fructose overfeeding derived from our metabolomics analysis showed distinct alterations. It can be deduced that metabolic alterations were associated with SFO, and a resilient metabolic response acted positively in SFO. For example, in response to SFO, plasma β-hydroxybutyrate and asparagine levels altered significantly. β-hydroxybutyrate can act as an indicator of energy balance, and can protect against oxidative stress as an endogenous histone deacetylase inhibitor [22, 23]. L-asparagine can improve energy status and inhibits AMP-activated protein kinase signaling pathways [24, 25]. From the resulting metabolic network, we can infer that a significant number of endogenous small molecules take part in SFO metabolic adaptions. Due to the active response of many endogenous molecules, metabolic homeostasis is maintained.

Moreover, to investigate potential mechanisms underlying *de novo* lipogenesis regulation, we also evaluated expression levels of ChREBP, SREBP-1 and SREBP-2 from the insulin-SREBP-1c (sterol regulatory element binding protein-1c) and the ChREBP (Carbohydrate Responsive-Element Binding Protein) pathways. In addition to the RNA-Seq analysis, we also verified their mRNA expression by qRT-PCR (Figure 4E). The results showed that the mRNA expression of ChREBP and SREBP-2 were

not influenced by SFO. Similarly, cholesterol metabolism was not influenced by SFO, consistent with previous literature [26, 27] indicating that SREBP-2 is responsible for regulating cholesterol biosynthesis. In contrast, SREBP-1 expression was downregulated (Figure 4E). Our western blotting results also confirmed this notable finding (Figure 8). As is well known, SREBP1 is bound to ER and cleaved in the Golgi before exerting its effects in regard to transcription in the nucleus. Here, down-regulation of expression of the larger uncleaved form of SREBP1 was demonstrated. This data suggests the existence of negative feedback regulation of SREBP-1; this mechanism could be partly responsible for resilient metabolic adaption to short-term fructose overfeeding.

4 Discussion

It has been demonstrated that long-term high fructose feeding causes increases in chronic liver inflammation, oxidative stress and fibrosis [1]. Here we also uncovered related negative consequences associated with SFO, based on both phenotypic change and biochemical examination. Our collective omics analysis here provides compelling evidence that SFO can induce a surprisingly rapid dyslipidemia. Moreover, IPA network analyses provided unique insights into metabolic stress in liver accompanying SFO in rats; linked with the isolated differentially expressed genes (DEGs) and significantly different metabolites (DMs) to generate the top most-stressed molecular networks, and predicted the most likely consequent conditions. Hypothesizing the aforementioned effects exist, a schematic model of short-term fructose overconsumption-induced metabolic disturbances and consequences is shown in Figure 9.

Although the focus of the present study was on hepatic and serum metabolic alteration, it should be acknowledged that the effects of fructose are not solely dependent upon its effects on the liver. Rather there are several lines of evidence suggesting that a major trigger of the fructose-dependent induction of NAFLD is through it´s effects on intestinal barrier function [28-30]. Meanwhile, fructose metabolism in the gut also plays a complex role in the process. Do et al. found that the high fructose-fed mice lost gut microbial diversity, characterized by a lower proportion of Bacteroidetes and a markedly increased proportion of Proteobacteria [31]. Crescenzo et al. reported that obesity and insulin

resistance are elicited by a high-fructose diet in adult rats [32]. Jena et al. reported a high-fructose diet induces inflammation and metabolic dysregulation in the gut and liver due to alterations in gut microbial communities [33].

4.1 Hepatic genes expression networks suffered from short-term fructose overfeeding

In the present study, significant alterations in expression of genes involved in hepatic *de novo* lipogenesis were observed in the livers of SFO rats. In turn, it was this not surprising that hepatic lipid accumulation and dysregulation of plasma total cholesterol were detected. A significant downregulation in liver PTGER2 mRNA expression shows its important role in metabolic adaption regulation after short-term fructose overconsumption. PTGER2, a crucial mediator of many physiological and pathological events [34], plays a key role in improving angiogenesis and subsequently adipogenesis, and metabolic disorders like hyperlipidemia and diabetes occur in underweight chronic obstructive pulmonary disease patients [35, 36]. Also of note was up-regulated expression of mRNA for trypsin family serine proteases with SFO, which also reveals the potential importance of these genes in the development of metabolic disturbances. For example, there existed an obvious increase in liver of PRSS1, PRSS2 and PRSS3 transcripts, which encode a series of highly similar proteins, namely, trypsinogen 1, 2, and 3. It has been reported that all of these are associated with chronic pancreatitis [37-40]. In addition, much higher expression of CEL, a carboxyl ester lipases involved in cholesterol biosynthesis and fat digestion and absorption, was also observed. CEL can interact with cholesterol and oxidized lipoproteins to modulate the progression of atherosclerosis [41, 42]. In our study, pancreatic triglyceride lipase (PNLIP), which is essential for dietary fat digestion in children and adults, was significantly up-regulated, as were two other homologs, pancreatic lipase-related protein 1 (PNLIPRP1) and pancreatic lipase-related protein 2 (PNLIPRP2). An altered lipid metabolism network, including key lipolytic enzymes PNLIP, PNLIPRP1 and PNLIPRP2, will affect

homeostasis of FFAs, and it has been proved that decreased gene expressions of these lipases leads to reduced FFAs in pancreatic tumors [8]. The above finding suggested that the surplus energy yield accompanying SFO leads to dyslipidaemia, potentially obesity. Inhibition of the activity of pancreatic lipase could prevent chronic impairments in the metabolic disorder. Similarly, here, fibroblast growth factor 21 (FGF21), an endocrine hormone that regulates energy homeostasis, also showed significant up-regulation. FGF21 concentration in plasma is increased in patients with obesity, insulin resistance, and metabolic syndrome [43, 44]. Our finding coincided with the aforementioned literature which revealed that fructose can activate hepatic transcription factor ChREBP, resulting in stimulation of hepatic FGF21 expression [45, 46]. It's reported that ChREBP is crucial for mediating fructose-induced metabolic adaptations [27] , but our results supported that SREBP-1 expression may actually be more sensitive in response to SFO.

4.2 Resilient metabolic regulation is instinctive in respond to short-term fructose overfeeding

Using multivariate statistical analysis, OPLS-DA provided the primary finding from GC-MS metabolic profiling that SFO led to acute alterations in the plasma metabolome, where concentrations of many endogenous small molecules were altered. Previous work has shown that facing metabolic stress, complicated but precise metabolic adjustments are launched almost simultaneously [47]. Resilient regulation appears to be an inherent response also to SFO, and our data provide some initial insights into some of the significant molecules involved. For instance, the obvious increase of plasma citrulline and itaconate level suggests their potential important role in SFO metabolic adaption. Citrulline is a non-essential amino acid and *in-vivo* studies have demonstrated it can attenuate the development of western-diet or high-fructose induced non-alcoholic fatty liver disease [7]. Citrulline appears to act directly on hepatic lipid metabolism by partially preventing hypertriglyceridemia and

steatosis through decreasing fatty acid synthase gene expression, probably via its action on the expression of the transcription factor sterol regulatory element binding protein-1c (SREBP-1c), a key regulator of hepatic *de novo* lipogenesis [48-50]. Here, our data was consistent with these studies. Moreover, there probably existed a citrulline-linked negative feedback regulation of SREBP-1, which contributed to resilience. In addition, a significantly altered concentration of plasma citrulline may be an indicator of SFO metabolic stress. Itaconate is another interesting molecule which can reduce visceral fat by inhibiting fructose 2,6-bisphosphate synthesis in rat liver [51]. Itaconate is validated as a mammalian metabolite induced during macrophage activation [52] and which can act as regulatory mediator of the inflammatory response; it regulates succinate levels, mitochondrial respiration, and cytokine production [53]. Our data also suggests that a significantly un-regulated itaconate accumulation may be due to the chronic inflammatory reactions occurring during SFO; it may thus be regarded as a candidate biomarker of SFO metabolism disturbance.

Moreover, there are also some other molecules we noted that are related to the development of hyperlipidemia, obesity, and non-alcohol fatty liver disease. For example, deoxycholic acid, L-tryptophan, taurine, mannitol and 3-hydroxybutyric acid were all significantly up-regulated in SFO rats. According to the literature, tryptophan can reduce the levels of pro-inflammatory cytokines and may be of benefit for patients with nonalcoholic fatty liver disease [54]; D-mannitol can suppress aspartate aminotransferase activity and reduce hepatic mitochondrial lipid peroxidation [55]. It is also interesting that lowering deoxycholic acid concentrations may mitigate vascular calcification in chronic kidney disease [56]. Taurine can improve obesity-induced inflammatory responses and modulates the unbalanced phenotype of adipose tissue macrophages [57]. 3-hydroxybutyric acid is a ketone body and acts as an indicator of energy balance and a central regulator of energy homeostasis,

and 3-hydroxybutyric acid can protect against oxidative stress as an endogenous histone deacetylase inhibitor [23].

Changes in all the aforementioned endogenous small molecules may reflect that SFO promotes a widespread attack on the normal rat metabolic network, requiring significant effort by resilience mechanisms to adapt to the metabolic stress. It can be expected that once the tolerable limits if this resilience is exceeded, high fructose intake associated metabolic disturbance will contribute to hyperlipidemia, obesity and non-alcohol fatty liver disease risk. Therefore, we propose that a focus on maintaining resilience would be a promising way to prevent and treat metabolic disorder-like conditions. Collectively, the distinct hepatic gene expression patterns and disordered metabolic networks occurring during SFO echoed the phenotypic changes at the transcriptome and metabolome levels respectively. Omics evidence supported that SFO disturbed metabolic homeostasis and that endogenous small molecules positively mediated SFO metabolic adaption. However, this metabolic regulation is clearly highly complex and other underlying mechanisms probably exist and should provide a fruitful area for further more detailed studies.

5 Conclusions

Using an integrated metabolomics and transcriptomics analyses, the present study provides a systematic omics insight into the consequences of SFO. The results provide further evidence that SFO induces major metabolic stress. We also identified negative feedback regulation of hepatic SREBP-1 mRNA and protein expression as a potential underlying mechanism playing an active role in regulating hepatic *de novo* lipogenesis while mediating SFO metabolic adaption. IPA molecular network analysis of the data showed that SFO can disturb metabolic homeostasis, but that inherent resilience mechanisms exist that might be targeted as an effective measure for preventing the development of

hyperlipidemia, obesity, and even diabetes. Moreover, endogenous metabolites and genes sensitive to SFO revealed in this study present meaningful clues for discovering and evaluating molecular biomarkers or gene targets underlying metabolic diseases, to underpin further physiopathological and pharmacological research.

Author Contributions

L.K., Y. M., H. Z-R. and W.Q. performed the experiments and analyzed the data. R. X. and G. J. designed experiments and supervised the project. L.K. wrote the manuscript. H. Z-B. and J.E.T. revised and improved the manuscript. All authors were involved in discussion of the results and reviewed the manuscript.

Acknowledgments

The work was supported in part by the National Natural Science Foundation of China [grant number 81530102] and Science and Technology Planning Project of Guangdong Province, China [grant number 2015A050502050 & 2016B050501003].

Competing financial interests

The authors declare no competing financial interests.

References

[1] S. A. Hannou, D. E. Haslam, N. M. McKeown and M. A. Herman, J. Clin. Invest. **2018**, *128*, 545.

[2] R. M. Pereira, J. D. Botezelli, K. C. da Cruz Rodrigues, R. A. Mekary, D. E. Cintra, J. R. Pauli, A. S. R. da Silva, E. R. Ropelle, L. P. de Moura, Nutrients, **2017**, *9*, 405.

[3] L. Tappy, K. A. Le, Physiol. Rev. **2010**, *90*, 23.

[4] L. C. Dolan, S. M. Potter, G. A. Burdock, Crit. Rev. Food Sci. Nutr. **2010**, *50*, 889.

[5] L. C. Dolan, S. M. Potter, G. A. Burdock, Crit. Rev. Food Sci. Nutr. **2010**, *50*, 53.

[6] K. L. Teff, J. Grudziak, R. R. Townsend, T. N. Dunn, R. W. Grant, S. H. Adams, N. L. Keim, B. P. Cummings, K. L. Stanhope, P. J. Havel, J. Clin. Endocrinol. Metab. **2009**, *94*, 1562.

[7] J. A. Welsh, A. J. Sharma, L. Grellinger, M. B. Vos, Am. J. Clin. Nutr. **2011**, *94*, 726.

[8] G. Zhang, P. He, H. Tan, A. Budhu, J. Gaedcke, B. M. Ghadimi, T. Ried, H. G. Yfantis, D. H. Lee, A. Maitra, N. Hanna, H. R. Alexander, S. P. Hussain, Clin. Cancer Res. **2013**, *19*, 4983.

[9] S. Rauschert, O. Uhl, B. Koletzko, F. Kirchberg, T. A. Mori, R. C. Huang, L. J. Beilin, C. Hellmuth, W. H. Oddy, J. Clin. Endocrinol. Metab. **2016**, *101*, 871.

[10] H. Hinterwirth, C. Stegemann, M. Mayr, Circ. Cardiovasc. Genet. **2014**, *7*, 941.

[11] Q. Y. Xu, Y. H. Liu, Q. Zhang, B. Ma, Z. D. Yang, L. Liu, D. Yao, G. B. Cui, J. J. Sun, Z. M. Wu, Acta Pharmacol. Sin. **2014**, *35*, 1265.

[12] K. Anjani, M. Lhomme, N. Sokolovska, C. Poitou, J. Aron-Wisnewsky, J. L. Bouillot, P. Lesnik, P. Bedossa, A. Kontush, K. Clement, I. Dugail, J. Tordjman, J. Hepatol. **2015**, *62*, 905.

[13] M. D. Roberts, C. B. Mobley, R. G. Toedebush, A. J. Heese, C. Zhu, A. E. Krieger, C. L. Cruthirds, C. M. Lockwood, J. C. Hofheins, C. E. Wiedmeyer, H. J. Leidy, F. W. Booth, R. S. Rector, BMC Gastroenterol. **2015**, *15*, 151.

[14] P. Porras, M. Duesbury, A. Fabregat, M. Ueffing, S. Orchard, C. J. Gloeckner, H. Hermjakob, Proteomics. **2015**, *15*, 1390.

[15] D. M. van Leeuwen, M. Pedersen, L. E. Knudsen, S. Bonassi, M. Fenech, J. C. Kleinjans, D. G. Jennen, Mutagenesis. **2011**, *26*, 27.

[16] J. I. Fenton, N. P. Nunez, S. Yakar, S. N. Perkins, N. G. Hord, S. D. Hursting, Diabetes Obes. Metab. **2009**, *11*, 343.

[17] K. Li, Z. He, X. Wang, M. Pineda, R. Chen, H. Liu, K. Ma, H. Shen, C. Wu, N. Huang, T. Pan, Y. Liu, J. Guo, Free Radic. Biol. Med. **2018**, *124*, 163.

[18] J. Xia, D. S. Wishart, Curr. Protoc. Bioinformatics. **2016**, *55*, 141011.

[19] B. Geidl-Flueck, P. A. Gerber, Nutrients. **2017**, *9*, 1026.

[20] W. Yue, C. S. Yang, R. S. DiPaola, X. L. Tan, Cancer Prev. Res. (Phila). **2014**, *7*, 388.

[21] A. Wegner, J. Meiser, D. Weindl, K. Hiller, Curr. Opin. Biotechnol. **2015**, *34*, 16.

[22] Y. H. Youm, K. Y. Nguyen, R. W. Grant, E. L. Goldberg, M. Bodogai, D. Kim, D. D'Agostino, N. Planavsky, C. Lupfer, T. D. Kanneganti, S. Kang, T. L. Horvath, T. M. Fahmy, P. A. Crawford, A. Biragyn, E. Alnemri, V. D. Dixit, Nat. Med. **2015**, *21*, 263.

[23] J. C. Newman, E. Verdin, Diabetes Res. Clin Pr. **2014**, *106*, 173.

[24] X. Wang, Y. Liu, S. Li, D. Pi, H. Zhu, Y. Hou, H. Shi, W. Leng, Br. J. Nutr. **2015**, *114*, 553.

[25] H. Huang, S. Vandekeere, J. Kalucka, L. Bierhansl, A. Zecchin, U. Bruning, A. Visnagri, N. Yuldasheva, J. Goveia, B. Cruys, K. Brepoels, S. Wyns, S. Rayport, B. Ghesquiere, S. Vinckier, L. Schoonjans, R. Cubbon, M. Dewerchin, G. Eelen, P. Carmeliet, EMBO J, **2017**, *36*, 2334.

[26] J. D. Horton, J. L. Goldstein, M. S. Brown, J. Clin. Invest. **2002**, *109*, 1125.

[27] D. Zhang, X. Tong, K. VanDommelen, N. Gupta, K. Stamper, G. F. Brady, Z. Meng, J. Lin, L. Rui, M. B. Omary, L. Yin, J. Clin. Invest. **2017**, *127*, 2855.

[28] K. Nomura, T. Yamanouchi, J. Nutr. Biochem. **2012**, *23*, 203.

[29] A. Spruss, I. Bergheim, J. Nutr. Biochem. **2009**, *20*, 657.

[30] C. Sellmann, J. Priebs, M. Landmann, C. Degen, A. J. Engstler, C. J. Jin, S. Garttner, A. Spruss, O. Huber, I. Bergheim, J. Nutr. Biochem. **2015**, *26*, 1183.

[31] M. H. Do, E. Lee, M. J. Oh, Y. Kim, H. Y. Park, Nutrients, **2018**, *10*. 761.

[32] R. Crescenzo, A. Mazzoli, , B. Di Luccia, F.Bianco, R. Cancelliere, L. Cigliano, G. Liverini, L. Baccigalupi, S. Iossa, Food Nutr. Res. **2017**, *61*, 1331657.

[33] P. K. Jena, S. Singh, B. Prajapati, G. Nareshkumar, T. Mehta, S.Seshadri, Appl. Biochem. Biotechnol. **2014**, *172*, 3810.

[34] J. Jiang, R. Dingledine, Trends Pharmacol. Sci. **2013**, *34*, 413.

[35] T. Tsuji, K. Yamaguchi, R. Kikuchi, M. Itoh, H. Nakamura, A. Nagai, K. Aoshiba, Prostaglandins Other Lipid Mediat. **2014**, *112*, 9.

[36] T. Tsuji, K. Yamaguchi, R. Kikuchi, H. Nakamura, R. Misaka, A. Nagai, K. Aoshiba, Prostaglandins Other Lipid Mediat. **2017**, *130*, 16.

[37] J. Oiva, O. Itkonen, R. Koistinen, K. Hotakainen, W. M. Zhang, E. Kemppainen, P. Puolakkainen, L. Kylanpaa, U. H. Stenman, H. Koistinen, Clin Chem, **2011**, *57*, 1506.

[38] M. J. Giefer, M. E. Lowe, S. L. Werlin, B. Zimmerman, M. Wilschanski, D. Troendle, S. J. Schwarzenberg, J. F. Pohl, J. Palermo, C. Y. Ooi, V. D. Morinville, T. K. Lin, S. Z. Husain, R. Himes, M. B. Heyman, T. Gonska, C. E. Gariepy, S. D. Freedman, D. S. Fishman, M. D. Bellin, B. Barth, M. Abu-El-Haija, A. Uc, J. Pediatr. **2017**, *186*, 95.

[39] X. Xiao, A. Mukherjee, L. E. Ross, M. E. Lowe, J. Biol. Chem. **2011**, *286*, 26353.

[40] K. Johnson, L. Ross, R. Miller, X. Xiao, M. E. Lowe, Pediatr. Res. **2013**, *74*, 127.

[41] D. Gilham, E. D. Labonte, J. C. Rojas, R. J. Jandacek, P. N. Howles, D. Y. Hui, J. Biol. Chem. **2007**, *282*, 24642.

[42] A. Kodvawala, A. B. Ghering, W. S. Davidson and D. Y. Hui, J. Biol. Chem. **2005**, *280*, 38592.

[43] A. Morovat, G. Weerasinghe, V. Nesbitt, M. Hofer, T. Agnew, G. Quaghebeur, K. Sergeant, C. Fratter, N. Guha, M. Mirzazadeh, J. Poulton, J. Clin. Med. **2017**, *6*, 80.

[44] R. Maekawa, Y. Seino, H. Ogata, M. Murase, A. Iida, K. Hosokawa, E. Joo, N. Harada, S. Tsunekawa, Y. Hamada, Y. Oiso, N. Inagaki, Y. Hayashi, H. Arima, J. Nutr. Biochem. **2017**, *49*, 71.

[45] J. R. Dushay, E. Toschi, E. K. Mitten, F. M. Fisher, M. A. Herman, E. Maratos-Flier, Mol. Metab. **2015**, *4*, 51.

[46] F. M. Fisher, M. Kim, L. Doridot, J. C. Cunniff, T. S. Parker, D. M. Levine, M. K. Hellerstein, L. C. Hudgins, E. Maratos-Flier, M. A. Herman, Mol. Metab. **2017**, *6*, 14.

[47] C. M. Metallo and M. G. Vander Heiden, Mol. Cell. **2013**, *49*, 388.

[48] N. Joffin, A. M. Jaubert, S. Durant, J. Bastin, J. P. De Bandt, L. Cynober, C. Moinard, C. Forest, P. Noirez, Mol. Nutr. Food. Res. **2014**, *58*, 1765.

[49] P. Jegatheesan, S. Beutheu, G. Ventura, E. Nubret, G. Sarfati, I. Bergheim, J. P. De Bandt, J. Nutr. **2015**, *145*, 2273.

[50] P. Jegatheesan, S. Beutheu, K. Freese, A. J. Waligora-Dupriet, E. Nubret, M. J. Butel, I. Bergheim, J. P. De Bandt, Br. J. Nutr. **2016**, *116*, 191.

[51] A. Sakai, A. Kusumoto, Y. Kiso, E. Furuya, Nutrition, **2004**, *20*, 997.

[52] C. L. Strelko, W. Lu, F. J. Dufort, T. N. Seyfried, T. C. Chiles, J. D. Rabinowitz, M. F. Roberts, J. Am. Chem. Soc. **2011**, *133*, 16386.

[53] V. Lampropoulou, A. Sergushichev, M. Bambouskova, S. Nair, E. E. Vincent, E. Loginicheva, L. Cervantes-Barragan, X. Ma, S. C. Huang, T. Griss, C. J. Weinheimer, S. Khader, G. J. Randolph, E. J. Pearce, R. G. Jones, A. Diwan, M. S. Diamond, M. N. Artyomov, Cell Metab. **2016**, *24*, 158.

[54] K. Celinski, P. C. Konturek, M. Slomka, H. Cichoz-Lach, T. Brzozowski, S. J. Konturek, A. Korolczuk, J. Physiol. Pharmacol., **2014**, *65*, 75.

[55] H. Yamamoto, T. Watanabe, H. Mizuno, K. Endo, T. Hosokawa, A. Kazusaka, R. Gooneratne and S. Fujita, Free Radic. Biol. Med. **2001**, *30*, 547.

[56] A. Jovanovich, T. Isakova, G. Block, J. Stubbs, G. Smits, M. Chonchol, M. Miyazaki, Am. J. Kidney Dis. **2017**, *71*, 27.

[57] S. Lin, S. Hirai, Y. Yamaguchi, T. Goto, N. Takahashi, F. Tani, C. Mutoh, T. Sakurai, S. Murakami, R. Yu and T. Kawada, Mol. Nutr. Food Res. **2013**, *57*, 2155.

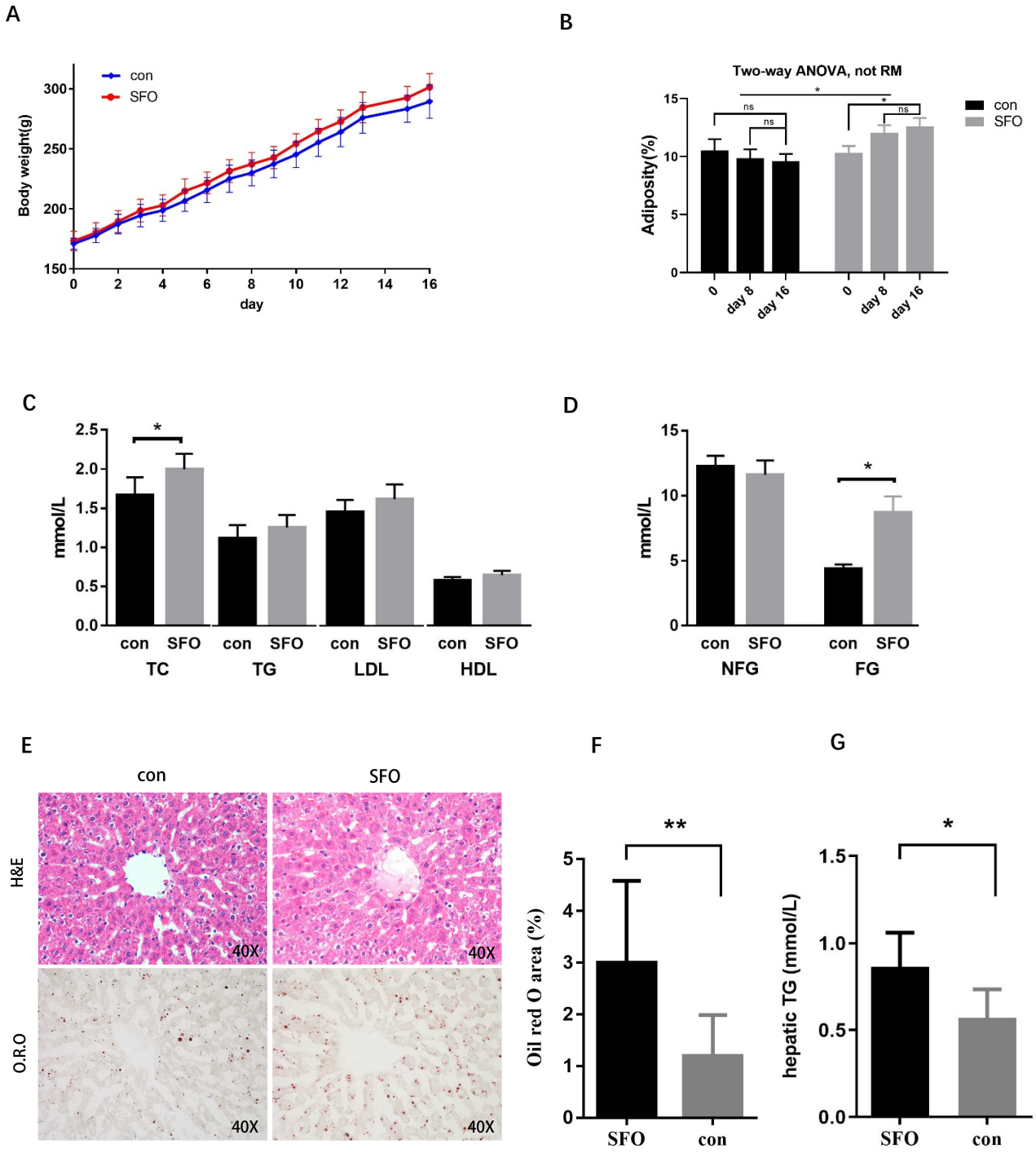

Figure 1: Short-term fructose overfeeding leads rapidly to dyslipidemia. The control group (con; n=6) and short-term fructose overfeeding group (SFO; n=6)) rats were measured for body weight **(A)** and adiposity **(B)**. Plasma lipid levels **(C)** and glucose levels **(D)** were also measured. Liver tissue sections were stained by H&E and O.R.O and imaged by microscopy (representative samples shown; ×40 magnification) **(E)**. Relative O.R.O stained plaque areas were quantitated using image J software **(F)**, hepatic TG levels were also measured **(G)**. Data are presented as mean ± SD (n=6), **p*<0.05, ***p*<0.01. TC, total cholesterol; TG, triglycerides; LDL-C, low-density lipoprotein cholesterol; HDL-C, high-density lipoprotein cholesterol. NFG, non-fasting glucose; FG, fasting glucose.

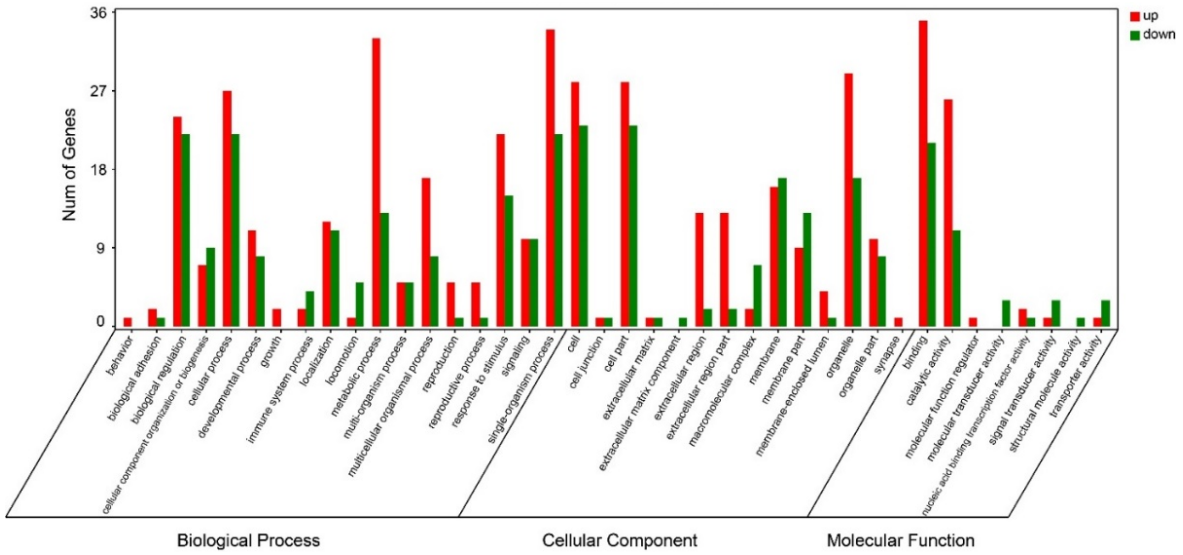

Figure 2: Gene Ontology classifications of differentially expressed genes between short-term fructose overfeeding group (SFO) and control group rats. Based on sequence homology, 105 differentially expressed genes could be categorized into three main categories (biological process, cellular component, and molecular function); these included 18, 14, and 8 functional groups, respectively.

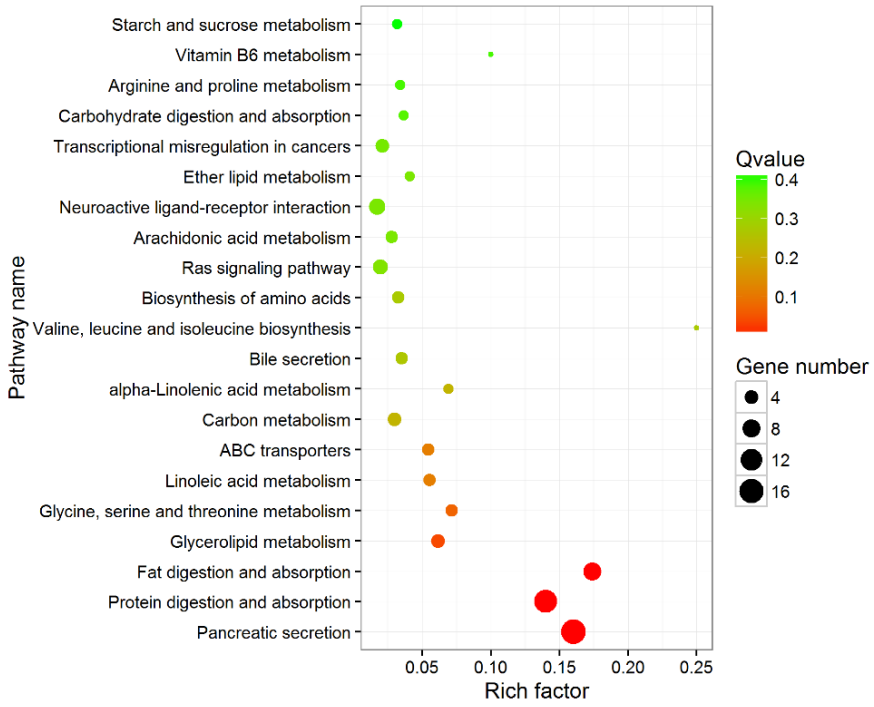

Figure 3: Top 20 enriched pathways of differentially expressed genes between the short-term fructose overfeeding and control group rats. The Y-axis on the left represents KEGG pathways, and the X-axis indicates the enrichment factor. Low Q-values are shown in red, and high Q-values in green.

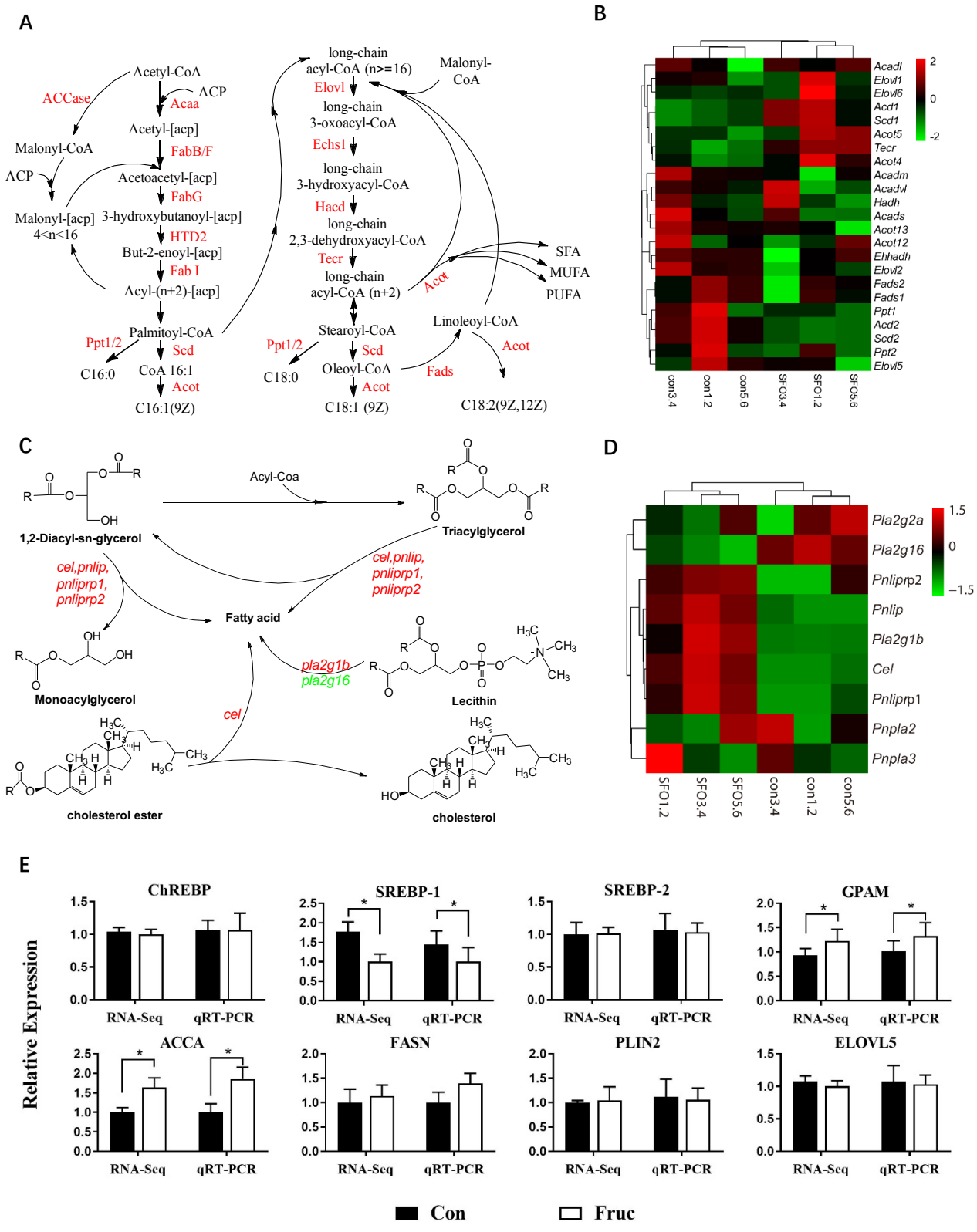

Figure 4: Hepatic lipogenesis gene expression is disturbed by short-term fructose overfeeding. **(A, C)** The schematic shows *de novo* lipogenesis pathways and acyl generating pathways in liver cells respectively. **(B, D)** Heatmaps display the expression of genes involved in the *de novo* biosynthesis pathway and acyl generating pathway respectively. **(E)** The relative mRNA expression level of several genes involved in lipogenesis was examined by qRT-PCR to validate RNA-Seq data. *ACCase,* Acetyl-

CoA carboxylease. *Acca,* Acetyl CoA acyltransferase. *Acads,* short-chain specific acyl-CoA dehydrogenase, mitochondrial precursor. *Acadm,* medium-chain specific acyl-CoA dehydrogenase, mitochondrial precursor. *Acadl,* long-chain specific acyl-CoA dehydrogenase, mitochondrial precursor.*Ppt1,* palmitoyl-protein thioesterase 1 precursor. *Ppt2,* palmitoyl-protein thioesterase 2. *Fads2,*fatty acid desaturase 2. *Fads1,* fatty acid desaturase 1.*tecr,* very-long-chain enoyl-CoA reductase. *Acd1,* acyl-CoA desaturase 1. *Acd2,* acyl-CoA desaturase 2. *Acot12,* acyl-coenzyme A thioesterase 12. *Acot13,* acyl-coenzyme A thioesterase 13. *Acot5,* acyl-coenzyme A thioesterase 5. *Acot4,* acyl-coenzyme A thioesterase 4. *Acadvl,*Acyl-Coenzyme A dehydrogenase, very long chain. *Hadh,*hydroxyacyl-coenzyme A dehydrogenase, mitochondrial precursor.*Elovl1,e*longation of very long chain fatty acids protein 1. *Elovl2,*elongation of very long chain fatty acids protein 2. *Elovl5,* elongation of very long chain fatty acids protein 5. *Elovl6,* elongation of very long chain fatty acids protein 6. *Pecr,*peroxisomal trans-2-enoyl-CoA reductase. *Scd1,* acyl-CoA desaturase 1. *Scd2,* acyl-CoA desaturase 2. *Cel*, carboxyl ester lipase. *Pnlip*, pancreatic lipase. *Pnliprp1*, pancreatic lipase-related protein 1. *Pnliprp2*, pancreatic lipase related protein 2. *Pnpla2*, patatin-like phospholipase domain containing 2. *Pnpla3*, patatin-like phospholipase domain containing 3. *Pla2g2a*, phospholipase A2 group IIA. *Pla2g1b*, phospholipase A2 group IB. *Pla2g16*, phospholipase A2, group XVI. *Srebp-1*, sterol regulatory element binding protein 1; *Srebp-2*, sterol regulatory element binding transcription factor 2; *Chrebp*, carbohydrate responsive-element binding protein.

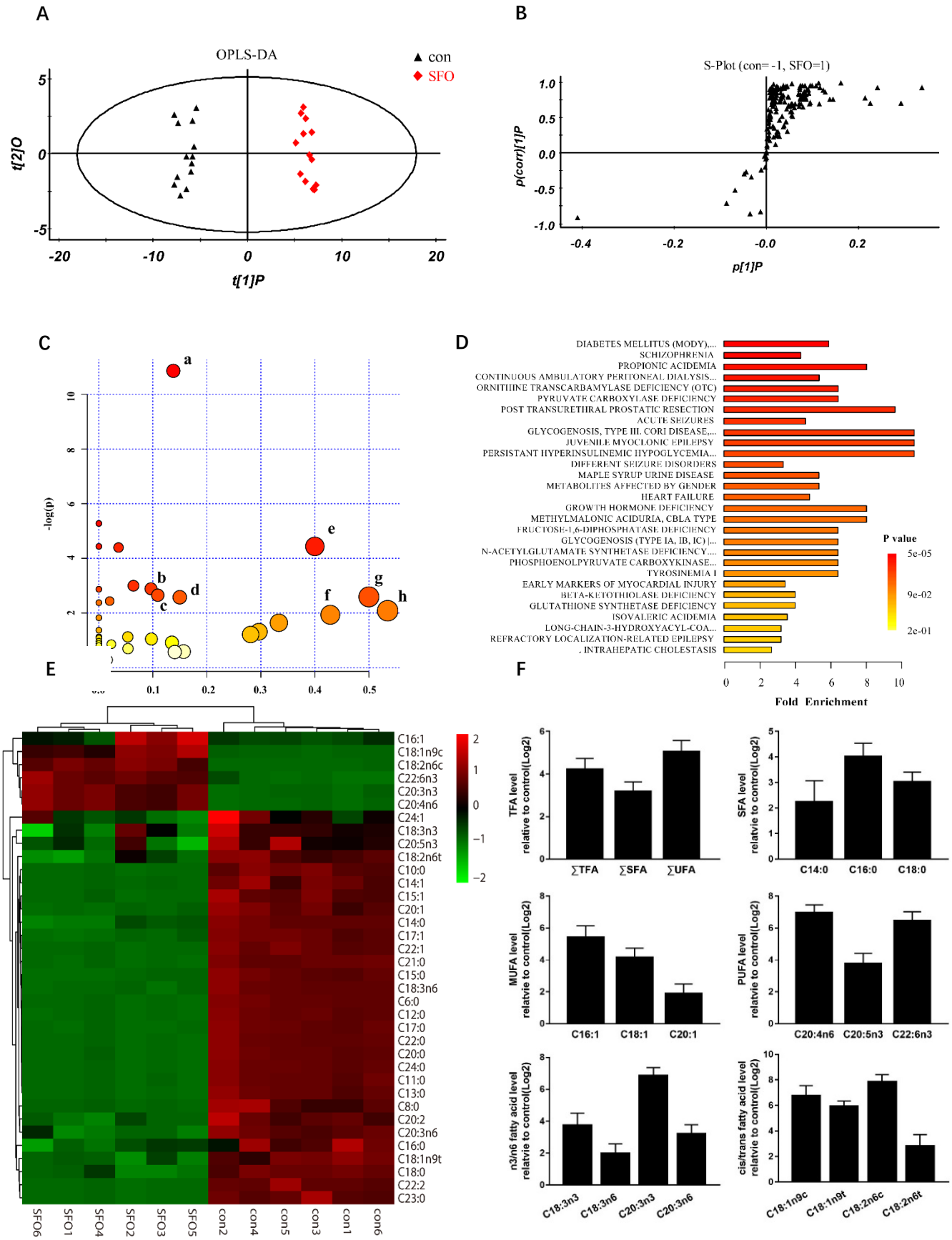
A
OPLS-DA
con
SFO
t[2]O
t[1]P
B
S-Plot (con= -1, SFO=1)
p(corr)[1]P
p[1]P
C
-log(p)
a
b
c
d
e
f
g
h
D
DIABETES MELLITUS (MODY),...
SCHIZOPHRENIA
PROPIONIC ACIDEMIA
CONTINUOUS AMBULATORY PERITONEAL DIALYSIS...
ORNITHINE TRANSCARBAMYLASE DEFICIENCY (OTC)
PYRUVATE CARBOXYLASE DEFICIENCY
POST TRANSURETHRAL PROSTATIC RESECTION
ACUTE SEIZURES
GLYCOGENOSIS, TYPE III, CORI DISEASE,...
JUVENILE MYOCLONIC EPILEPSY
PERSISTANT HYPERINSULINEMIC HYPOGLYCEMIA...
DIFFERENT SEIZURE DISORDERS
MAPLE SYRUP URINE DISEASE
METABOLITES AFFECTED BY GENDER
HEART FAILURE
GROWTH HORMONE DEFICIENCY
METHYLMALONIC ACIDURIA, CBLA TYPE
FRUCTOSE-1,6-DIPHOSPHATASE DEFICIENCY
GLYCOGENOSIS (TYPE IA, IB, IC) |...
N-ACETYLGLUTAMATE SYNTHETASE DEFICIENCY,...
PHOSPHOENOLPYRUVATE CARBOXYKINASE...
TYROSINEMIA I
EARLY MARKERS OF MYOCARDIAL INJURY
BETA-KETOTHIOLASE DEFICIENCY
GLUTATHIONE SYNTHETASE DEFICIENCY
ISOVALERIC ACIDEMIA
LONG-CHAIN-3-HYDROXYACYL-COA...
REFRACTORY LOCALIZATION-RELATED EPILEPSY
, INTRAHEPATIC CHOLESTASIS
P value
5e-05
9e-02
2e-01
Fold Enrichment
E
C16:1
C18:1n9c
C18:2n6c
C22:6n3
C20:3n3
C20:4n6
C24:1
C18:3n3
C20:5n3
C18:2n6t
C10:0
C14:1
C15:1
C20:1
C14:0
C17:1
C22:1
C21:0
C15:0
C18:3n6
C6:0
C12:0
C17:0
C22:0
C20:0
C24:0
C11:0
C13:0
C8:0
C20:2
C20:3n6
C16:0
C18:1n9t
C18:0
C22:2
C23:0
SFO6
SFO1
SFO4
SFO2
SFO3
SFO5
con2
con4
con5
con3
con1
con6
F
TFA level relative to control(Log2)
∑TFA
∑SFA
∑UFA
SFA level relative to control(Log2)
C14:0
C16:0
C18:0
MUFA level relative to control(Log2)
C16:1
C18:1
C20:1
PUFA level relative to control(Log2)
C20:4n6
C20:5n3
C22:6n3
n3/n6 fatty acid level relative to control(Log2)
C18:3n3
C18:3n6
C20:3n3
C20:3n6
cis/trans fatty acid level relative to control(Log2)
C18:1n9c
C18:1n9t
C18:2n6c
C18:2n6t

Figure 5: Non-targeted metabolomics (NTM) and quantitative targeted lipidomics analysis (QTLA) of rat plasma from control and SFO rats. (A) OPLS-DA plot of GC-MS profiling of high-fructose intake group and control group plasma, R^2Y=0.9896, Q^2=0.9844. **(B)** S-plot of OPLS-DA analyzed by SIMCA-P 12 (Umetrics, Umeå, Sweden). **(C)** Summary of pathway analysis with MetaboAnalyst 3.0; (a) Aminoacyl-tRNA biosynthesis; (b) Primary bile acid biosynthesis; (c) galactose metabolism; (d) Alanine, aspartate and glutamate metabolism; (e) Methane metabolism; (f) Taurine and hypotaurine metabolism; (g) Phenylalanine, tyrosine and tryptophan biosynthesis; (h) Glycine, serine and threonine metabolism. **(D)** Quantitative enrichment analysis performed using the metabolites set enrichment analysis with MetaboAnalyst 3.0. **(E**) Heatmap of 36 fatty acid species alteration calculated by normalization method. Red shading indicates upregulation and green indicates downregulation. **(F**) Relative levels of some significantly altered plasma fatty acids. The total fatty acid (TFA), saturated fatty acid (SFA), unsaturated fatty acid (UFA), monounsaturated fatty acid (MUFA), polyunsaturated fatty acid (PUFA), n3 or n6 fatty acid and *cis*-or *trans*- fatty acid were calculated on the 36 fatty acid profiles respectively.

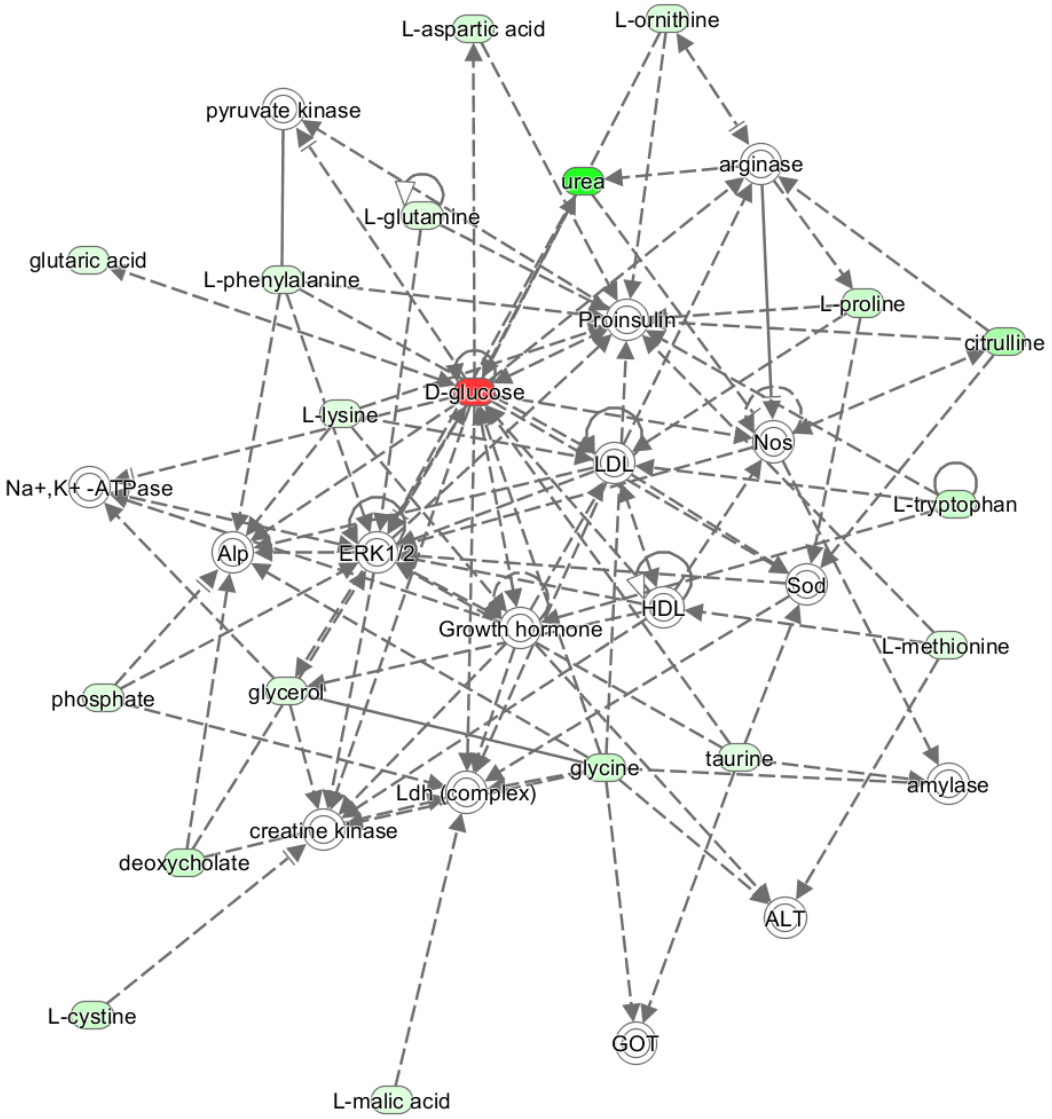

Figure 6: Top regulated metabolic network in short-term fructose overfeeding group rats (IPA score 47). Molecules in red were up-regulated while those in green were down-regulated (control group versus short-term fructose overfeeding group). LDL-C, low-density lipoprotein; HDL-C, high-density lipoprotein. ERK1/2, extracellular regulating kinase 1/2; Nos, nitric oxide synthase. Sod, superoxide dismutase; ALT, alanine aminotransferase; GOT, glutamic oxalacetic transaminase; Ldh, lactate dehydrogenase.

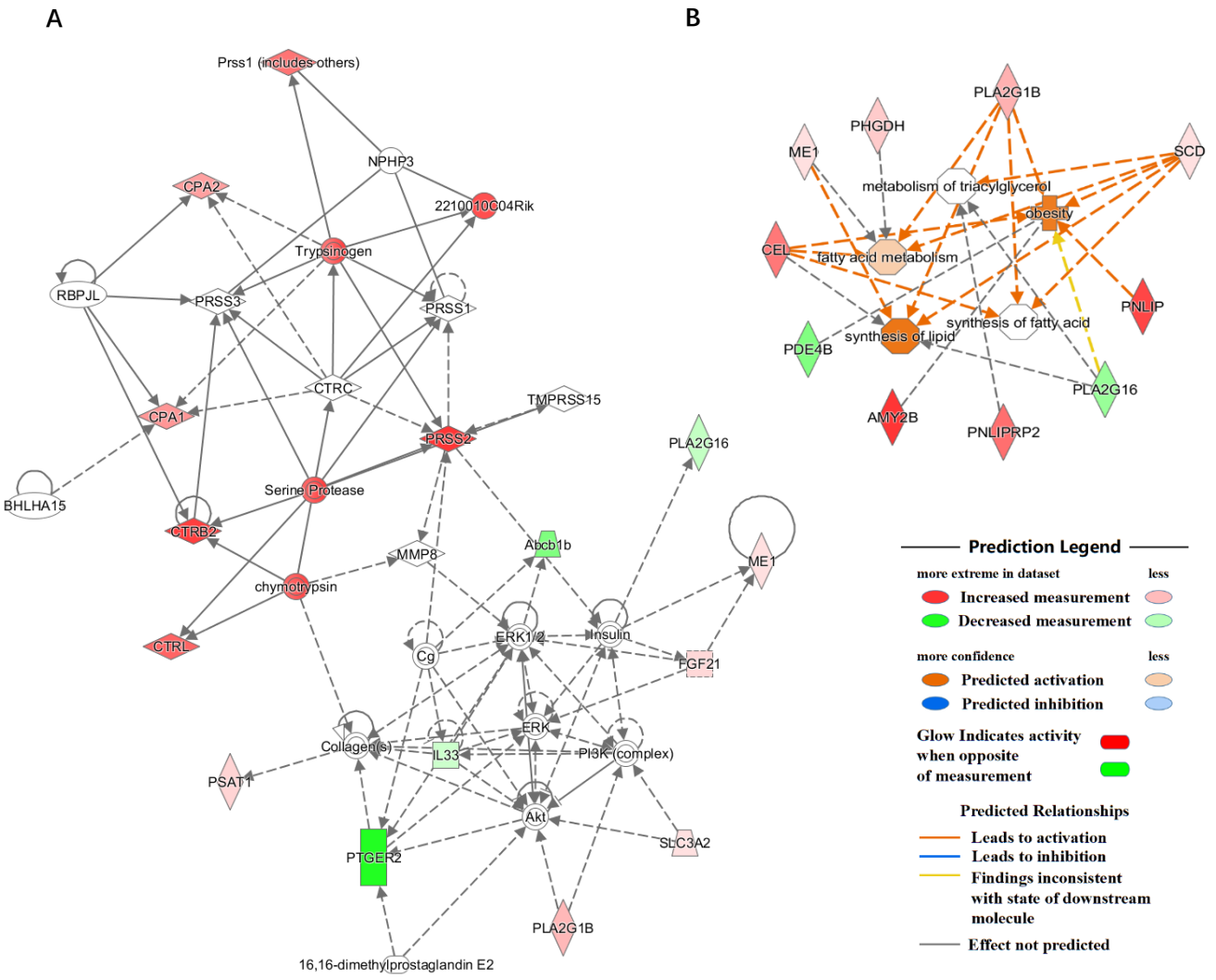

Figure 7: Molecular network of differentially-expressed genes between short-term fructose overfeeding rats and control rats using IPA. (A) Analysis based on top network with IPA score 40. **(B)** Intensive sub-network from (A) related to glycolipids metabolism in high-fructose intake group rats. Molecules in red were up-regulated while those in green were down-regulated (short-term fructose overfeeding group versus control group). *Pla2g16*, phospholipase A2, group XVI; *Me1*, malic enzyme 1; *Fgf21*, fibroblast growth factor 21; *Slc3a2*, solute carrier family 3 member 2; *Pla2g1b*, phospholipase A2, group IB; *Ptger2*, prostaglandin E receptor 2; *Psat1*, phosphoserine aminotransferase 1; *Il33*, interleukin 33; *Abcb1b*, ATP-binding cassette, subfamily B (MDR/TAP), member 1B; *Mmp8*, matrix metallopeptidase 8; *Ctrl*, chymotrypsin-like; *Ctrb2*, chymotrypsinogen B2; *Prss1*, protease, serine, 1; *Prss2*, protease, serine, 2; *Tmprss15*, transmembrane protease, serine 15; *Ctrc*, chymotrypsin C; *Cpa1*, carboxypeptidase A1; *Prss3*, protease, serine, 3; *Cpa2*, carboxypeptidase A2; 2210010C04Rik, RIKEN cDNA 2210010C04 gene; *Nphp3*, nephrocystin 3; *Rbpjl*, recombination signal binding protein for immunoglobulin kappa J region-like; *Bhlha15*, basic helix-loop-helix family, member a15; *Scd*, stearoyl-CoA desaturase (delta-9-desaturase); *Pnlip*, pancreatic lipase; *Pnliprp2*, pancreatic lipase related protein 2; *Amy2b*, amylase 2b; *Pde4b*, phosphodiesterase 4B; *Cel*, carboxyl ester lipase; *Phgdh*,phosphoglycerate dehydrogenase.

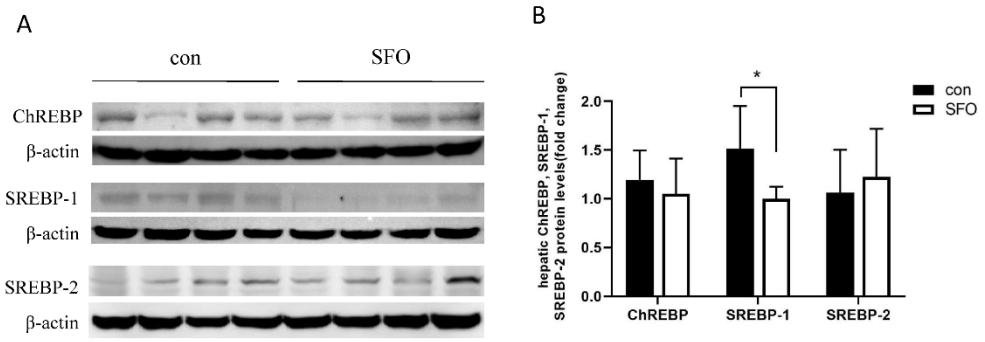

Figure 8: Self-adaptive regulation of hepatic ChREBP, SREBP-1 and SREBP-2 expression in response to short-term fructose overfeeding. Representative western blots (4 samples per group) are shown; β-actin levels were used as a loading control (A). Bar graphs show densitometry analysis of specific bands expressed as fold change (B). The values are given as mean ± SD (n = 6 each).*$p < 0.05$.

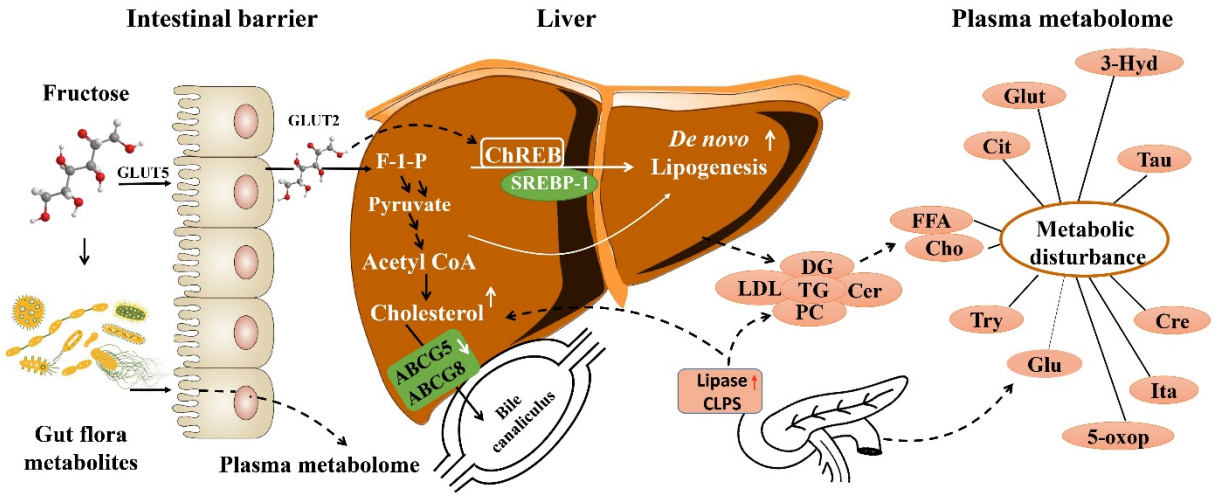

Figure 9: Schematic illustration of metabolic disturbances and their consequences induced by short-term fructose overconsumption. GLUT5, glucose transporter 5; GLUT2, glucose transporter 2;F-1-P, fructose-1-phosphate; Glu, D-Glucose; Cit, citrulline; 3-Hyd, 3-Hydroxybutyric acid; Tau, taurine; Glut, L-glutamine; Try, L-tryptophan; Cre, creatinine; Ita, itaconate; 5-oxop, 5-oxoproline; FFA, free fatty acids; Cho, cholesterol; DG, diacylglycerol; TG, triglycerides; LDL, low-density lipoprotein; PC, phosphatidylcholine; CLPS, colipase; Cer, ceramide; SREBP-1, sterol regulatory element binding protein 1; ChREBP, carbohydrate responsive-element binding protein.